

# Antithrombin-Independent Effects of Heparins on Fibrin Clot Nanostructure

Christelle Yeromonahos,\* Raphaël Marlu,\* Benoît Polack, Francois Caton

**Objective**—Because of the widespread clinical use of heparins, their effects on the enzymatic cascade are very well known. In contrast, little is known about the direct effect of heparins on the nanostructure of fibrin fibers, even though this nanostructure plays a major role in the mechanical strength and lysis of clots. This lack of reliable data can be correlated with the lack of a noninvasive, quantitative method to determine this structure. We recently developed such a method that allows the simultaneous determination of the average fiber radius and the protein content using spectrometric data. In this study, we assessed the nanostructure of fibrin in a system composed of human thrombin and fibrinogen.

**Methods and Results**—We provide quantitative evidence showing that both unfractionated heparin and low molecular weight heparin directly alter the nanostructure of fibrin fibers independent of their other actions on the coagulation cascade; as expected, the pentasaccharide fondaparinux has no effect.

**Conclusion**—Our results show that in addition to the effect of heparin on the coagulation cascade, modifications of the fibrin nanostructure may also contribute to improved fibrinolysis. (*Arterioscler Thromb Vasc Biol.* 2012;32:1320-1324.)

**Key Words:** fibrin fibers ■ fondaparinux ■ low-molecular-weight heparin ■ nanostructure ■ spectrophotometry ■ unfractionated heparin

Fibrin fibers, the primary structural components of blood clots, polymerize as a consequence of coagulation at sites of vascular injury. Serving as a scaffold to promote wound healing, the fibrin gel must withstand the shear forces exerted by flowing blood, which is why the remarkable elasticity of fibrin is crucial for its biological function. Indeed, the structural and mechanical properties of fibrin clots are particularly important for understanding, preventing, and treating thrombosis.<sup>1-3</sup> As recently demonstrated,<sup>4</sup> the nanostructure of fibrin fibers plays a major role in the mechanical strength of fibrin clots, but, to maintain hemostasis and minimize the impact of thrombosis, fibrin fibers must be porous enough to allow plasmin to lyse the clots.

Determining the fibrin nanostructure is a difficult task because of the typical radii of the fibers (~100 nm) and because of the extremely hydrated nature of the fibers. However, there are few methods for the noninvasive and quantitative measurement of the nanostructure of fibrin fibers. Among these methods, the small-angle neutron scattering (SANS) and X-ray scattering (SAXS) techniques provide absolute structural information; however, such large-scale instruments cannot be regularly used. Alternatively, dynamic and static light scattering and turbidimetry yield measurements that are in agreement with SANS or SAXS results, in contrast with the results of electron microscopy (EM). Indeed, under similar conditions, the average diameter of fibrin fibers estimated by turbidimetry and light-scattering techniques<sup>5-8</sup> is 3 times

larger than that observed via EM.<sup>9-12</sup> Because electron beams are strongly absorbed by water, EM measurements are made using clots that are nearly dry. Because the solvent content of fibrin fibers is at least 80%, EM measurements are qualitatively related to the actual amount of protein in the fibers but not to the true size of the fibers themselves and are dependent on the drying protocol used.<sup>13</sup>

Using SAXS data for validation of our results, we recently developed a spectrometric method that enables the simultaneous determination of the average fiber radii, the number of protofibrils per fiber, the interprotofibril distance, and the protein content inside the fibers.<sup>14</sup>

Numerous studies since the 1930s have shown that clot structures depend on their microenvironment (eg, ionic strength, pH, and the presence of anticoagulant molecules).<sup>14-18</sup> Despite the widespread clinical use of various heparins and the precise knowledge of their effect on the coagulation cascade, their effects on fibrin fiber structure have not been thoroughly elucidated. Some studies<sup>19-32</sup> have investigated the influence of unfractionated heparins (UFH), low-molecular-weight heparins (LMWH), and the pentasaccharide fondaparinux on the structure of the fiber in the absence of antithrombin. In the presence of UFH, the fibrin network is more porous and is composed of thicker fibers.<sup>19-22,31</sup> However, some data suggest that the fiber sizes are reduced at a sufficiently high concentration of

Received on: March 4, 2011; final version accepted on: February 10, 2012.

From Laboratoire de Rhéologie, CNRS UMR5520, Université Joseph Fourier, Grenoble, France (C.Y., F.C.); Laboratoire d'Hématologie, CHU, Grenoble, France (R.M., B.P.); and Laboratoire TIMC-IMAG/TheREx, CNRS UMR5525, Université Joseph Fourier, Grenoble, France (R.M., B.P.).

\*C.Y. and R.M. contributed equally to this work.

Correspondence to Prof. Benoît Polack, Hématologie Biologique CHU de Grenoble BP 217, F-38043 Grenoble Cedex 9 France. E-mail BPolack@chu-grenoble.fr

© 2012 American Heart Association, Inc.

*Arterioscler Thromb Vasc Biol* is available at <http://atvb.ahajournals.org>

DOI: 10.1161/ATVBAHA.112.245308

UFH.<sup>19,31,32</sup> The effects of LMWH are more contradictory and are probably due to the differences in the experimental conditions. It is unclear whether LMWH has no effect on clot structure<sup>20,22</sup> or is responsible for reducing fiber size.<sup>24</sup> In addition, it was shown that the addition of fondaparinux to purified fibrinogen before clotting did not induce a modification of the clot structure.<sup>25</sup> Therefore, there is a clear need to characterize the effects of heparins on the nanostructure of fibrin fibers.

We addressed this issue using a simplified system that consisted of purified human fibrinogen and thrombin, and our data provide quantitative evidence that UFH and LMWH alter the nanostructure of fibrin fibers independent of their coagulation cascade effects.

## Methods

### Materials

Purified human fibrinogen was a generous gift from the Laboratoire Français du Fractionnement et des Biotechnologies (LFB, Les Ulis, France). Human thrombin was purchased from Cryopep (Montpellier, France). UFH was obtained from Sanofi-Aventis (Paris, France). The LMWH enoxaparin and the synthetic pentasaccharide fondaparinux were purchased from Sanofi-Aventis and GlaxoSmith Kline (Marly-le-Roi, France), respectively. The concentrations of UFH and LMWH are presented in anti-Xa IU/mL, and the concentration of fondaparinux is in  $\mu\text{g/mL}$ . All of the solutions were stored at  $-80^\circ\text{C}$ .

### Preparation of Fibrin Gels

Before use, fibrinogen and thrombin aliquots were thawed at  $37^\circ\text{C}$  for 5 minutes. The aliquots were diluted in a HEPES buffer (0.14 mol/L NaCl, 20 mmol/L HEPES, pH 7.4) maintained at  $37^\circ\text{C}$ . The heparins were diluted in the same buffer and maintained at  $37^\circ\text{C}$  at 4 times the final concentration. To initiate the polymerization, 0.5 mL of the thrombin solution was added to 0.25 mL of the fibrinogen solution and 0.25 mL of the heparin solution. For the control experiments, the heparin solution was replaced by buffer. The clots were formed directly in 10-mm-thick polystyrene cuvettes from a mixture that typically contained 1 mg/mL fibrinogen, 1.25 IU/mL thrombin, and 0.005–50 anti-Xa IU/mL heparins (or 0.5–500  $\mu\text{g/mL}$  of fondaparinux). All of the clots were formed at  $37^\circ\text{C}$  for 90 minutes. The cuvettes were covered with Parafilm to prevent evaporation.

### Spectrophotometric Evaluation of the Final Clot Nanostructure

The average mass-to-length ratio ( $\mu$ ) and radius ( $a$ ) of the fibrin fibers were determined by the method described by Yeromonahos et al.<sup>14</sup> The number of protofibrils per cross section was determined from the  $\mu$  alone, using the formula  $N_p = \mu/\mu_0$ , where  $\mu_0 = 1.44 \times 10^{11}$  Da/cm represents the mass/length ratio of a single protofibril. The average protein mass concentration in the fibers is represented by  $\delta = \mu/(\pi a^2)$ , and the average distance between the protofibrils is represented by  $z = (\mu_0/\delta)^{0.5}$ .

Each data point in all of the graphs represent at least 3 individual clotting experiments. The corresponding standard deviations were calculated from these replicates.

### Evaluation of the Quantity of Fibrinopeptide A Release From Fibrinogen

Fibrin clots were formed at  $37^\circ\text{C}$  for 90 minutes in 1 mL aliquots. The fibrin was then wound on a glass rod, and the supernatant was centrifuged for 20 minutes at 15000g and then assayed by ELISA (ZYMUTEST FPA, Hyphen Biomed, Neuville sur Oise, France).<sup>33</sup> The results are expressed as the percentage of fibrinopeptide A (FPA) released relative to the total amount of FPA available, as calculated from the initial fibrinogen concentration.

### Fluorescent Determination of Thrombin Activity

The thrombin activity was measured in separate experiments, using the same reagents and a Fluoroskan Ascent microplate reader in the fluorimetric mode. A simplified CAT technique<sup>34</sup> was used to determine the activity of thrombin. ZZGR-AMC (210  $\mu\text{mol/L}$  final concentration) was added to each well to a solution containing a final concentration of 1 mg/mL fibrinogen, 1.25 IU/mL IIa, and varying concentrations of UFH or LMWH. The evolution of the fluorescence was followed after automated mixing of the reagents. The low concentrations of the reagents and the low recorded intensities ensure that the inner filter effect can be neglected. Thus, the recorded intensity is directly proportional to the concentration in the produced AMC. From these data, the maximum slope of each curve is extracted ( $S_m$ ), which is proportional to the true maximum velocity ( $V_m$ ) of the enzymatic reaction of thrombin with ZZGR-AMC. Hence, the ratio of  $S_m$  to the maximum slope without heparin ( $S_{m_0}$ ) is equal to the  $V_m/V_{m_0}$  ratio. In other words,  $S_m/S_{m_0}$  is equal to the true activity of thrombin in solution relative to the activity of thrombin in the absence of heparin.

## Results

### Thrombin Activity: The Presence of Traces of Antithrombin in the Purified Fibrinogen

Despite using affinity chromatography on heparin Sepharose in the purification process of the fibrinogen and the absence of detection of antithrombin by standard clinical laboratory assays, our preliminary results indicated the possible presence of residual traces of antithrombin in the fibrinogen. Therefore, the inhibitory activity of the antithrombin present in the fibrinogen preparation was measured using a fluorimetric method (described in the Methods section) in the presence of various concentrations of heparin. The fluorimetric curves in Figure 1A and 1B showed that the thrombin activity is indeed strongly reduced by the addition of heparin. The relative thrombin activity is plotted in Figure 2 and shows a factor of 5 between the catalytic efficiencies of UFH and LMWH on the inhibition of thrombin by antithrombin, in good agreement with the literature.<sup>35</sup> The coherence of this determination is further evaluated by computing the amount of FPA that should be released during the course of this enzymatic reaction and comparing this amount with the actual measurements made when adding different quantities of UFH. The inset of Figure 2 shows that the fluorimetric method gives results that are in good agreement with the FPA measurements.

### Structure of the Fibers With Varying Concentrations of Thrombin

Because UFH and LMWH have antithrombin-mediated thrombin-inhibition effects, we thus evaluated the influence of variations in the thrombin concentration on the nanostructure of the fibrin fibers. To this end, we measured, in the absence of heparins, the structural parameters of the fibrin fibers as a function of the thrombin concentration using our spectrometric method.

Figure 3 shows the presence of an extremum in the fibers nanostructural parameters at 0.1 IU/mL of IIa. For instance, whereas the internal density of the fibers increases by 100% with increasing IIa concentration between 0.01 IU/mL and 0.1 IU/mL, it decreases by 60% when the IIa concentration is further increased. Similarly, the average radius of the fibers

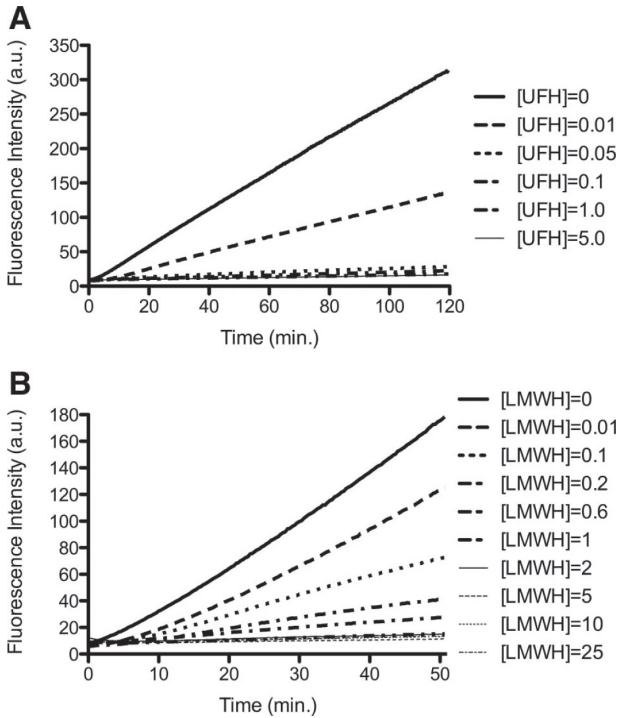


**Figure 1.** A, Cleavage of ZZGR-AMC by 1.25 IU/mL IIa in the presence of 1 mg/mL fibrinogen for various concentrations of unfractionated heparin (UFH). B, Cleavage of ZZGR-AMC by 1.25 IU/mL IIa in the presence of 1 mg/mL fibrinogen for various concentrations of low-molecular-weight heparin (LMWH).

initially increased from 87 nm to a maximum of 113 nm, but the radius returned to 87 nm in the presence of greater amounts of thrombin (data not shown).

From this curve, the structure can be deduced for a given thrombin activity. Therefore, we can discriminate between the structural modification due to the antithrombin-mediated inhibition and strictly heparin-dependent structural modifications.

### Antithrombin-Independent Effects of UFH on Fibrin Fiber Nanostructure

In Figure 4, the evolution of the internal density of the fibrin fibers is plotted against the UFH concentration; no

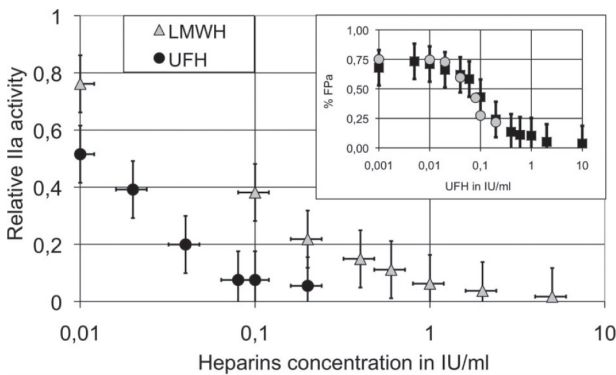


**Figure 2.** IIa relative activity at various unfractionated heparin (UFH, black circles) and low-molecular-weight heparin (LMWH, gray triangles) concentrations. Inset: Measured (black squares) and fluorescence-deduced (gray circles) FPA released after 90 minutes for various UFH concentrations.

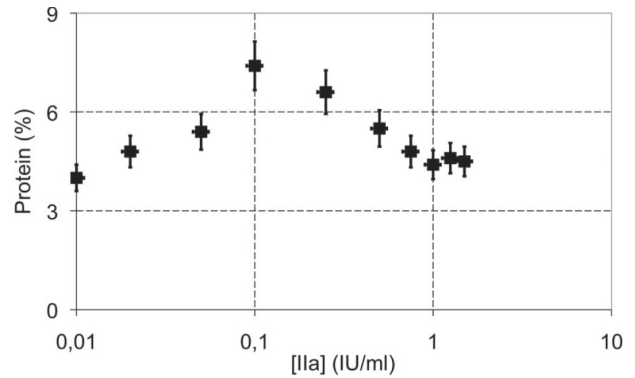


**Figure 3.** Nanostructure (protein content) of the fibrin fibers at various concentrations of IIa without heparin.

clots were observed for experiments performed using more than 0.2 IU/mL of UFH.

Below 0.1 IU/mL UFH, there are parallel increases in the observed (black squares) and predicted (gray triangles) fibrin fiber densities. This result agrees with previously reported turbidity measurements and electron microscopy observations,<sup>20,22</sup> which indicated that a low concentration of UFH resulted in more opaque and porous networks having thicker fibrin fibers. More quantitatively, the comparison between the observed and predicted structures shows that between 0 and 0.1 IU/mL of UFH, both the radius and the density are significantly lower than would be observed if the UFH had only a thrombin-inhibition effect. This result suggests a ternary interaction between fibrin, UFH, and thrombin at all concentrations.

At 0.2 IU/mL of UFH there is a very large discrepancy between the predicted structure and the observed structure. In this clot, the fibers were composed of only 25 protofibrils, which is indicative of an abnormal clot. Above that concentration, fibrin polymerization was completely inhibited.

We can conclude from these observations that for all concentrations, UFH directly increases the porosity of fibrin fibers.

### Antithrombin-Independent Effects of LMWH on Fibrin Fiber Nanostructure

In Figure 5, the nanostructure of the fibrin fibers is plotted as a function of the LMWH concentration. In contrast with the

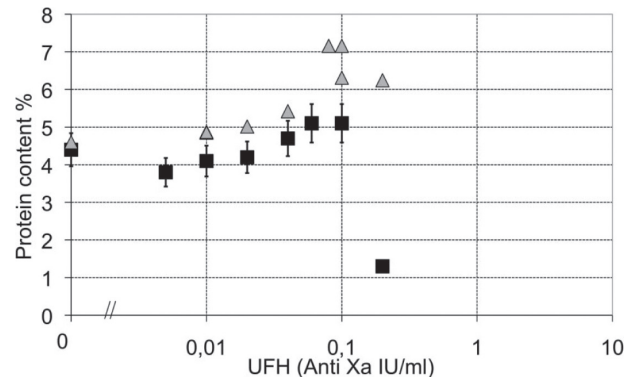


**Figure 4.** Nanostructure (protein content) of the fibrin fibers at various concentrations of unfractionated heparin (UFH). Black squares indicate measured; gray triangles, predicted.

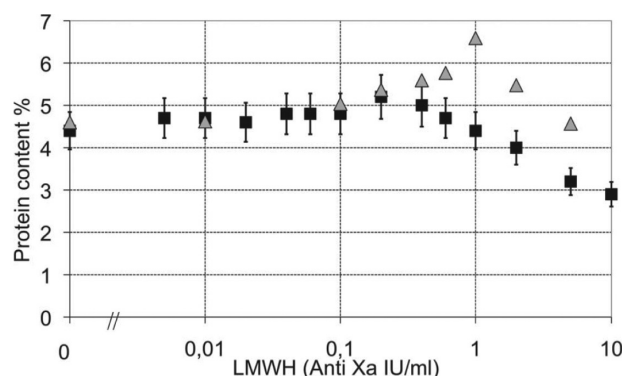


**Figure 5.** Nanostructure (protein content) of the fibrin fibers at various concentrations of low-molecular-weight heparin (LMWH). Black squares indicate measured; gray triangles, predicted.

UFH results, clots were obtained over a much larger range of concentrations. Here, the predicted and observed nanostructures are almost superimposed for LMWH <0.2 IU/mL. Looking closely at the data, there is a marginal decrease in the radius with increasing LMWH concentration, whereas the prediction shows a slight increase. However, this difference is almost within the error bars of the measurements. This is in good qualitative agreement with the findings of Parise et al,<sup>22</sup> who concluded that, at these concentrations, LMWH had little effect on the fiber nanostructure.

In contrast, there is a clear divergence between the 2 curves above a concentration of 0.4 IU/mL, revealing an interaction that is not attributable to the inhibition by thrombin. Increasing the LMWH leads to a very progressive 50% decrease in the protein content of the fibers, whereas the radius of the fibers slightly decreases. Between 1 IU/mL and 10 IU/mL, increasing the LMWH concentration contributed to the formation of increasingly porous fibrin fibers. Finally, fibrin polymerization was totally inhibited above 10 IU/mL of LMWH, that is, 2 orders of magnitude higher than the inhibiting concentration of UFH. These results are consistent with the significant decrease in turbidity observed by Carr and Powers.<sup>24</sup>

We can conclude from these observations that LMWH directly and greatly increases the porosity of the fibrin fibers above a concentration of 0.2 IU/mL, whereas a clot is still formed up to concentrations of 10 IU/mL.

Concentrations of pentasaccharide up to 500 µg/mL had no effect on the fibrin fiber structure (data not shown). The number of protofibrils inside the fibers, the protein content of the fibers, the fiber radii and the interprotofibril distance remained independent of the fondaparinux concentration. These results agree with the findings of Varin<sup>25</sup> and Paolucci.<sup>29</sup>

## Discussion

The main finding of this study is that heparins influence the fibrin fiber nanostructure through both the antithrombin-mediated inhibition of thrombin and through a direct effect. This influence is essentially biphasic when either UFH or LMWH is present, as demonstrated by the structural modification at relatively low heparin concentrations and

the subsequent inhibition of fibrin polymerization at high heparin concentrations.

In the case of UFH, the inhibition at high concentrations should be related to the impediment of fibrin polymerization due to the formation of ternary complexes with fibrin, heparin, and thrombin, as shown by Hogg.<sup>26</sup> Analyzing our data with the Hogg formula,<sup>26</sup> we obtained a thrombin-to-heparin affinity constant of 9 nmol/L. Considering that these heparins are from different sources, our constant is in excellent agreement with a Hogg value of 15 nmol/L. The presence of such ternary complexes should also explain the increased porosity at low UFH concentrations, as it is probable that those ternary complexes are incorporated into the fibers.

The case of LMWH is even more interesting than that of UFH. Indeed, at very high concentrations of LMWH, the polymerization is inhibited, probably through the formation of ternary complexes. However, at intermediate concentrations, a profound modification of the structure, which cannot be explained by thrombin inhibition, is observed. We surmise that this could be the consequence of the incorporation of LMWH molecules into the fibers. Last, at low concentrations, only the expected structural modification due to the antithrombin-mediated thrombin inhibition is present.

In conclusion, it is of interest to highlight that the 2 regimens of nanostructure modification observed for both UFH and LMWH heparins correspond quite well to the 2 therapeutic regimens: prophylaxis and therapy.

## Sources of Funding

The authors are indebted to Dr Z. Tellier from LFB for funding the study.

## Disclosures

None.

## References

- Weisel JW. The mechanical properties of fibrin for basic scientists and clinicians. *Biophys Chem.* 2004;112:267–276.
- Collet JP, Soria J, Mirshahi M, Hirsch M, Dagonnet FB, Caen J, Soria C. Dusart syndrome: a new concept of the relationship between fibrin clot architecture and fibrin clot degradability: hypofibrinolysis related to an abnormal clot structure. *Blood.* 1993;82:2462–2469.
- Mosseson MW. Dysfibrinogenemia and thrombosis. *Semin Thromb Hemost.* 1999;25:311–319.
- Piechocka IK, Bacabac RG, Potters M, Mackintosh FC, Koenderink GH. Structural hierarchy governs fibrin gel mechanics. *Biophys J.* 2010;98:2281–2289.
- Carr ME, Hermans J. Size and density of fibrin fibers from turbidity. *Macromolecules.* 1978;11:46–50.
- Bernocco S, Ferri F, Profumo A, Cuniberti C, Rocco M. Polymerization of rod-like macromolecular monomers studied by stopped-flow, multiangle light scattering: set-up, data processing, and application to fibrin formation. *Biophys J.* 2010;98:2813–2826.
- Ferri F, Greco M, Arcovito G, Bassi FA, DeSpirito M. Growth kinetics and structure of fibrin gels. *Phys Rev E.* 2001;63:031401.
- Ferri F, Greco M, Arcovito G, DeSpirito M, Rocco M. Structure of fibrin gels studied by elastic light scattering techniques: dependence of fractal dimension, gel crossover length, fiber diameter and fiber density on monomer concentration. *Phys Rev E.* 2002;66:011913.
- Ryan EA, Mockros LF, Weisel JW, Lorand L. Structural origins of fibrin clot rheology. *Biophys J.* 1999;77:2813–2826.
- DeSpirito M, Arcovito G, Papi M, Rocco M, Ferri F. Small and wide angle elastic light scattering study of fibrin structure. *J Appl Cryst.* 2003;36:636–641.

11. Hantgan RR, Hermans J. Assembly of fibrin: a light scattering study. *J Biol Chem*. 1979;254:11272–11281.
12. Weisel JW. Fibrin assembly. Lateral aggregation and the role of the two pairs of fibrinopeptides *Biophys J*. 1986;50:85–13.
13. Hunziker EB, Straub PW, Haeberlis A. A new concept of fibrin formation based upon the linear growth of interlacing and branching polymers and molecular alignment into interlocked single-stranded segments. *J Biol Chem*. 1990;265:7455–7463.
14. Yeromonahos C, Polack B, Caton F. Nanostructure of the fibrin clot. *Biophys J*. 2010;99:2018–2027.
15. Choay J. Structure and activity of heparin and its fragments : an overview. *Semin Thromb Hemost*. 1989;15:359–364.
16. Hirsh J, Raschke R. Heparin and low-molecular-weight heparin: the seven ACCP conference on antithrombotic and thrombolytic therapy. *Chest*. 2004;126:188S–203S.
17. Ferry JD, Morrison PR. Preparation and properties of serum and plasma proteins: the conversion of human fibrinogen to fibrin under various conditions. *J Am Chem Soc*. 1947;69:388–399.
18. Shulman S, Ferry JD, Tinoco I. The conversion of fibrinogen to fibrin XII: influence of pH, ionic strength and hexamethylene glycol concentration on the polymerization of fibrinogen. *Arch Biochem Biophys*. 1953;42:245–256.
19. Jung H, Tae G, Kim YH, Johannsmann D. Change of viscoelastic property and morphology of fibrin affected by antithrombin III and heparin: QCM-Z and AFM study. *Colloids Surf B Biointerfaces*. 2009;68:111–119.
20. Collen A, Smorenburg SM, Peters E, Lupu F, Koolwijk P, Van Noorden C, van Hinsbergh VW. Unfractionated and low molecular weight heparin affect fibrin structure and angiogenesis in vitro. *Cancer Res*. 2000;60:6196–6200.
21. LeBoeuf RD, Gregg RR, Weigel PH, Fuller GM. Effects of hyaluronic acid and other glycosaminoglycans on fibrin polymer formation. *Biochemistry*. 1987;26:6052–6057.
22. Parise P, Morini M, Agnelli G, Ascani A, Nenci GG. Effects of low molecular weight heparins on fibrin polymerization and clot sensitivity to t-PA-induced lysis. *Blood Coagul Fibrinolysis*. 1993;4:721–727.
23. Sato H, Nakajima A, Shimohira T. Kinetic study on the initial stage of the fibrinogen-fibrin conversion by thrombin (IV): effects of heparin and its analogues. *Thromb Res*. 1985;39:549–557.
24. Carr ME, Powers PL. Effect of glycosaminoglycans on thrombin- and Atroxin-induced fibrin assembly and structure. *Thromb Haemost*. 1989;62:1057–1061.
25. Varin R, Mirshahi S, Mirshahi P, Kierzek G, Sebaoun D, Mishal Z, Vannier JP, Borg JY, Simoneau G, Soria C, Soria J. Clot structure modification by fondaparinux and consequence on fibrinolysis: a new mechanism of anti-thrombotic activity. *Thromb Haemost*. 2007;97:27–31.
26. Hogg PJ, Jackson CM. Heparin promotes the binding of thrombin to fibrin polymer: quantitative characterization of a thrombin-fibrin polymer-heparin ternary complex. *J Biol Chem*. 1990;265:241–247.
27. Hogg PJ, Jackson CM. Formation of a ternary complex between thrombin, fibrin monomer, and heparin influences the action of thrombin on its substrates. *J Biol Chem*. 1990;265:248–255.
28. Hogg PJ, Jackson CM, Labanowski JK, Bock PE. Binding of fibrin monomer and heparin to thrombin in a ternary complex alters the environment of the thrombin catalytic site, reduces affinity for hirudin, and inhibits cleavage of fibrinogen. *J Biol Chem*. 1996;271:26088–26095.
29. Paolucci F, Claviés MC, Donat F, Necciari J. Fondaparinux sodium mechanism of action: identification of specific binding to purified and human plasma-derived proteins. *Clin Pharmacokinet*. 2002;41:11–18.
30. Abildgaard U. Inhibition of the thrombin-fibrinogen reaction by heparin in absence of cofactor. *Scand J Haematol*. 1968;5:432–439.
31. Shinowara GY. Enzyme studies on human blood: interrelation of fibrin and fibrinogen fractions. *Am J Physiol*. 1949;156:458–466.
32. Godal HC. The influence of heparin on the fibrin clot. *Scand J Clin Lab Invest*. 1961;13:306–313.
33. Gralnick HR, Givelber HM, Finlayson JS. A new congenital abnormality of human fibrinogen: fibrinogen Bethesda II. *Thromb Diath Haemorrh*. 1973;29:563–571.
34. Hemker HK, Beguin S. Thrombin generation in plasma: its assessment via endogenous thrombin potential. *Thromb Haemost*. 1995;74:134–138.
35. Beguin S, Mardiguian J, Lindhout T, Hemker HC. The mode of action of low molecular heparin preparation (PK10169) and two of its major components on thrombin generation in plasma. *Thromb Haemost*. 1989;61:30–34.